

Abstract

In this report, we study the behaviour of the simple pendulum, as well as the numerical relations between the parameters of the function which governs its motion. A pendulum consisting of two strings supporting a weight to two independently fixed pivot points, designed in such a way as to allow the mass, length, and amplitude of the system to easily be altered, is used to collect all the data considered in this report. It is concluded that the angular amplitude depends on time periodically with an exponentially decaying envelope so long as the initial angular amplitude lies in the domain of $|\theta_0| < 0.25\text{rads}$. It is further concluded that the length of the pendulum dictates the observed period of oscillation as $T = 2\sqrt{\ell}$, where T is the period of oscillation and ℓ is the length of the pendulum. The decay coefficient, τ is observed to have quadratic relations depending on both the length and initial angular amplitude, while having logarithmic dependence on the mass m of the weight being used. Finally, a numerical estimation of the symmetry is underwent to conclude that the constructed pendulum has 98.7% symmetry, and by extension, implies strong correlation between the expected behaviour and the observed behaviour of the system.

Introduction

The pendulum is a thoroughly studied and well understood dynamical system which acts as a crucial learning experience for young physicists. This model provides an opportunity to further grasp and understand the importance of the small angle approximation not only in the physical sense, but also as a strong mathematical tool which can commonly be deployed to greatly simplify a problem. To set the stage for the theoretical framework which follows, let a point particle of mass m be suspended from a immovable pivot point by a massless string of length ℓ with negligible thickness. Define the value θ to be the angle that the string makes with the vertical line which passes through the pivot point. A schematic diagram of the system is included in Figure 1. The forces acting on the mass are the force due to gravity, the tangential component of such being given by $F_g = -mg \sin \theta$, as well as force due to wind resistance; drag. The magnitude of the drag force is proportional to the (tangential) velocity of the mass (which in this case is $\ell\dot{\theta}$): $F_d = \gamma\ell\dot{\theta}$, where γ is the constant of proportionality called the drag coefficient [Lea09]. Then Newton's second law provides;

$$m\ell\ddot{\theta} = -mg \sin \theta - \gamma\ell\dot{\theta} \quad (1)$$

Under the small angle approximation $\sin \theta \approx \theta$, Eq.(1) becomes

$$\ddot{\theta} + \frac{\gamma}{m}\dot{\theta} + \omega^2\theta = 0 \quad (2)$$

where $\omega = \sqrt{g/\ell}$. This is the equation that governs the motion of the damped pendulum under the small angle approximation. The general solution to Eq.(2), while stipulating that $\dot{\theta}(0) = 0$ and that the drag force is sufficiently small (namely, $(\gamma^2/m^2) \ll 1$), is given by

$$\theta(t) = \theta_0 e^{-t/\tau} \cos(\omega't) = \theta_0 e^{-t/\tau} \cos\left(\frac{2\pi t}{T}\right) \quad (3)$$

where $\omega' = \sqrt{\frac{g}{\ell} - \frac{\gamma^2}{2m^2}}$; the angular frequency, and $\tau = m/\gamma$; the decay coefficient [Ser13]. This implies that the rate of decay is independent of the initial amplitude, and remains constant in time. It is important to notice that a large value of γ results in a quickly decaying exponential $e^{-t/\tau}$, which aligns with physical intuition. Again assuming $\gamma^2 \ll m^2$, this provides that $\omega' \approx \omega$. Using the fact that the angular frequency is related to the period of oscillation by $\omega = 2\pi/T$, we can set

$$T = 2\pi\sqrt{\frac{\ell}{g}} \approx 2\sqrt{L+D} \quad (4)$$

Where we set $\ell = L + D$, L being the length of the string and D being the distance from the centre of mass to the point where the string is attached (which is non-zero for a physical pendulum). The relationship given by Eq.(4)

directly implies that the period of oscillation is independent of m and θ_0 , and stays constant throughout time. The goal of this paper is to test the accuracy of Eq.(3) and Eq.(4), analyze the dependence of the decay coefficient τ on m , ℓ , and θ_0 , and estimate a domain on which the small angle approximation remains valid through the use of a physical damped pendulum. Various physical limitations certainly arise in the construction of the pendulum, and as such, the symmetry of the pendulum is to be quantified. These dependencies will be quantified by constructing a physical pendulum, the motion of which will be tracked and analyzed over time. From the collected data, estimates on the various unknown quantities which appear in Eq.(3) will be derived, from which the validity of the theoretical claims mentioned above will be tested.

Finally, various uncertainty values will be computed from the collected data, all of which are propagated using the uncertainties in the dependent and independent variables alike. The uncertainty value, σ_F , of a function $F(x, y)$ is given by

$$\sigma_F^2 = \left(\frac{\partial F}{\partial x} \right) \sigma_x^2 + \left(\frac{\partial F}{\partial y} \right) \sigma_y^2 + 2 \frac{\partial F}{\partial x} \frac{\partial F}{\partial y} \sigma_{xy} \quad (5)$$

Where σ_x is the uncertainty in x and likewise for σ_y [Wik23]. Note that $\sigma_{xy} = \sigma_x \sigma_y \rho_{xy}$ is the covariance between the two values x and y , and ρ_{xy} the correlation between x and y . For the purposes of this experiment, the correlation is always taken to be 0.

Experimental Procedure

The numerical relations and values of interest, as discussed in the introduction, are estimated by varying three main independent variables: the mass m , the initial amplitude θ_0 , and the length of the string L . To obtain objective results, it is crucial that only one independent variable is altered at a time. The value $D = 0.004\text{m}$ holds true for all of the weights used in this experiment. The above theory relies on the fact that the mass is restricted to a two-dimensional plane of motion: the value of θ uniquely specifies the position of the mass at any given time. In an effort to do so, the method of Newton's cradle is deployed: the mass is held by *two* strings, attached to different pivot points. The two pivot points are in turn held stationary by metal posts that are firmly planted in place as to not move when undergoing measurements. Again, a schematic diagram of the system is included in Figure 1. To ensure symmetry in the motion of the mass, the strings must be attached to the pivot points in such a way that the length of the string remains constant throughout an entire period. To do so, hose clamps are used to hold the strings firmly in place on the metal poles. Due to how thin these hose clamps are and how firmly they grab onto the pole, the length of the pendulum remains constant, and hence the system act highly symmetrically. Ultimately, this ensures that the metal poles act as a clean hinge for the string to turn about. These minuscule details about the specifications of the system truly contribute to decreasing the uncertainties in each measurement, and by extension, improve the results themselves. The symmetry of the system, however, is further discussed and ultimately quantified in the results section of this report.

In total, 16 sets of data were collected, each of which includes at least 60 seconds of oscillation of the pendulum. Six (6) sets were collected while leaving the mass and length of the pendulum fixed at $m = 50\text{g}$, $L = 100\text{mm}$, and varying the initial angular amplitude of the mass. The actual numerical values of these initial amplitudes are of little importance so long as a breadth of values are used between 0 and $\pi/2$. With that being said, three of these data sets were taken with initial angular amplitude $\theta_0 < 0.20\text{rad}$. Similarly, five (5) sets were collected leaving the mass and initial angular amplitude fixed at $m = 100\text{g}$ and $\theta_0 = 0.22\text{rads}$, while varying the length of the string L . Keeping the mass fixed is rather simple, however the method used to fix θ_0 is to mark a location (that lies in the same plane as the pendulum's motion) on the supporting surface, and drop the mass in such a way that the string, if extended to the hit the surface, would intersect this point. Only after numerical analysis is the actual value of this θ_0 determined. This method is depicted nicely in the schematic diagram of the system, Figure 1. The lengths used in this data set are $L = 75\text{mm}, 100\text{mm}, 125\text{mm}, 150\text{mm}$ and 200mm . Finally, five (5) sets of data were collected leaving the length and initial angular amplitude fixed at $L = 100\text{mm}$ and $\theta_0 = 0.22\text{rads}$, while varying the

mass of the pendulum. The same method which was described above to leave θ_0 fixed is again used for this collection of data. The masses of the weights used in this collection are $m = 50\text{g}, 100\text{g}, 200\text{g}, 400\text{g}$, and 500g .

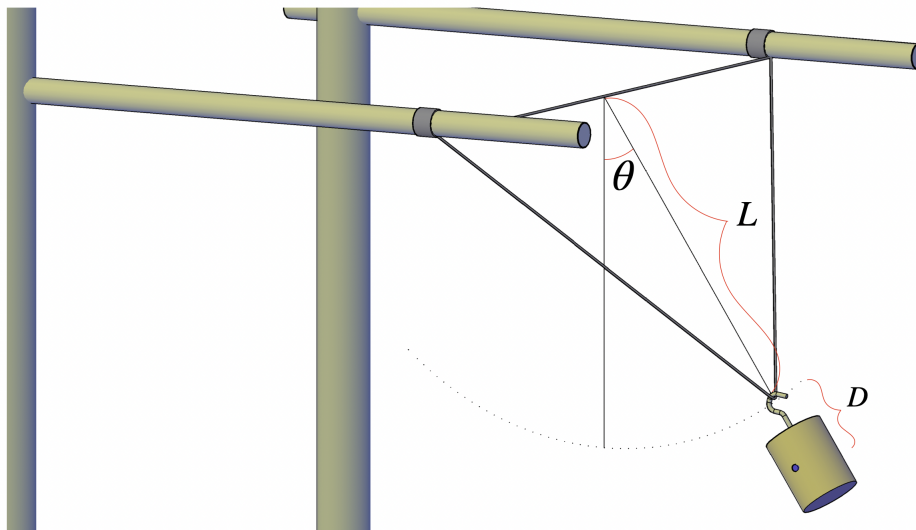


Figure 1: A 3d schematic diagram describing the system used to take all of the data for this report. It is labelled with the relevant variables, as well as a blue dot indicating the object used to optimize the tracking and data recording process.

The aforementioned sets of data are taken as an MP4 file using an iPhone, and imported to the application 'Tracker: Video Analysis and Modelling Tool'. Tracker uses automated RGB line profiling to record the position of an object at any given time [Tra09]. In order to truly exploit the full power and accuracy of this application, distinct variability between the colour of the object being tracked and the colour of the backdrop are essential prerequisites for obtaining clean and accurate results. As such, a piece of blue tape of approximately 5mm diameter is placed on the centre of mass of each weight used. This allows for Tracker to swiftly differentiate between the weight and any other object in the frame of the recording between time steps. With that being said, uncertainty in each recorded value arises due to the size of the tape being used: Tracker simply pinpoints a location that matches the previous RGB reading (up to 20% evolution), which leaves a 5mm variability between possible recordings. This variability (and resulting implications) is discussed in further detail in the uncertainty analysis section of the report. After recording the position of the weights at each time step, Tracker provides a three dimensional .txt file indicating the (x, y) coordinates of the weight at each time step. All of these files are imported to Python and fitted, using SciPy's `curve_fit`, to the functional form of Eq.(2). The values of θ_0 , T and τ are optimized to replicate the data as accurately as possible, values of which are then used to test the validity of the theoretical claims made in the introduction.

Uncertainty Analysis

Multiple sources of uncertainty come into play in the numerical analysis of this pendulum. Minor contributions arise from deviations in the length of the string throughout the motion of the mass. As to ensure a sufficiently large uncertainty is propagated for all combinations of the independent variables (in particular paying attention to the proportionality between the magnitude of the stretching and the mass of the object), it was measured that the string stretched a distance 2.00mm between a 20.00g mass (as to keep the string taught) and the 500.00g mass (the largest mass used), and therefore an uncertainty value of 2.00m is placed on the length of the string L . Other uncertainties may arise from motion of the pivot point, however the system used two large 30kg stands with broad bases, and no motion of either pivot point was visible throughout the experiment. As such, no additional uncertainty is propagated from this plausible source of error.

The largest source of uncertainty, however, arises from within the tracking methods themselves. As briefly discussed in the experimental procedure section of the report, Tracker pinpoints a *single* pixel on each frame, rather

then an entire object. Efforts to reduce this source of uncertainty were deployed by placing a small piece of tape at the centre of mass (from the perspective of the camera), however the size of the tape itself is certainly non-negligible. The same size of tape is used in each set of data, the diameter of which is 0.006m. It is assumed that the geometric centre of the tape is recorded on each frame, thus resulting in an uncertainty value of 0.003m in both the x and y coordinates. Using this value, the uncertainty in the angle θ is propagated using Eq.(5). Given values of x and y , the angle θ is then given by $\theta(x, y) = \ell \arctan\left(\frac{x}{y}\right)$, so that the uncertainty in θ is given by;

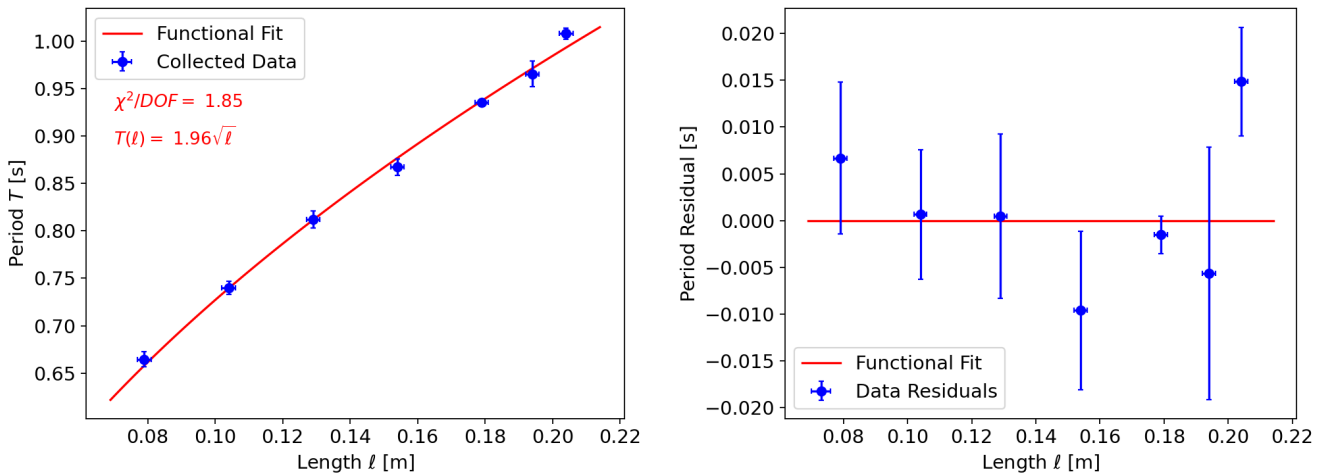
$$\sigma_\theta = \ell \sqrt{\frac{x^2 \sigma_x^2 + y^2 \sigma_y^2}{(x^2 + y^2)^2}} = \ell \sqrt{\frac{(0.003\text{m})^2}{x^2 + y^2}} \quad (6)$$

Note that the uncertainty in the value ℓ here is ignored, and such an approximation is justified since the only term involving such is $\sigma_\ell^2/\ell^2 \approx 0$. The error is applied to every data point in every data set, and has the largest magnitude over all other uncertainties making the tracking methods the largest source of uncertainty.

Results

Period of Oscillation T

As concluded from the theoretical considerations discussed in the introduction, it is hypothesized that the period of oscillation T is independent of the mass m , the initial angular amplitude θ_0 , and is related to the length of the string by Eq.(4). Figure 2a plots the estimated period of oscillation, optimized by `curve_fit` over the first 100 time steps, against their respective lengths ℓ for the five data sets with a fixed mass $m = 0.1\text{kg}$ and fixed initial angular amplitude $\theta_0 = 0.22\text{rads}$. The lengths used lie in the domain (0.075m, 0.20m) with the associated periods lying in the domain (0.65s, 1.00s). These data points are then fitted with a functional form $T = A\sqrt{\ell} = A\sqrt{L + D}$, with the proportionality constant taking on a value of $A = (1.96 \pm 0.09)[\text{s}/\sqrt{\text{m}}]$, a value which certainly has magnitude comparable to the hypothesized proportionality constant $A = 2$. The uncertainty propagation of A is done using the covariance matrix provided by `curve_fit`. The optimized fit carries a goodness of fit estimation of $\chi^2 = 1.85$; this indicates a strong correlation between the collected data and fitted functional form. Up to uncertainty, the expected value of the constant of proportionality, $A = 2[\text{s}/\sqrt{\text{m}}]$, and the computed value, $A = (1.96 \pm 0.09)[\text{s}/\sqrt{\text{m}}]$, are equal in value, and thus the validity of Eq.(4) is concluded.

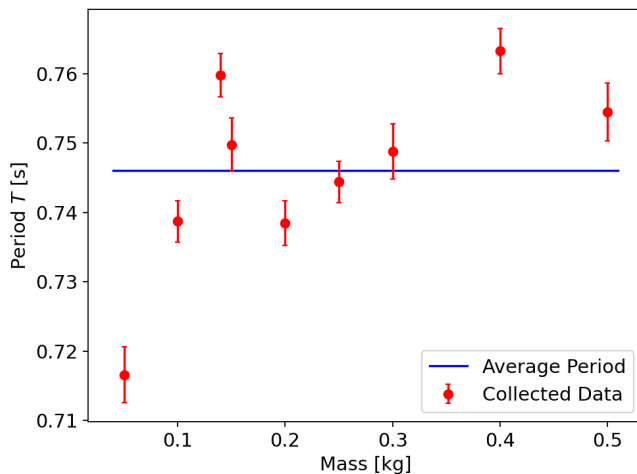


(a) Length versus estimated period of oscillation.

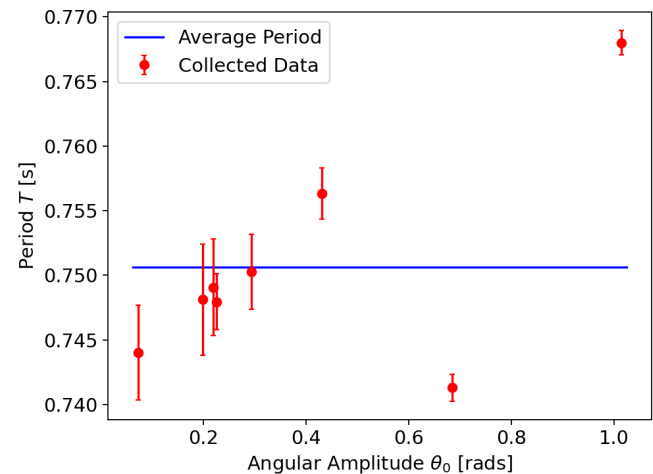
(b) Residuals of collected data versus optimized fit.

Figure 2: (Left) A plot of the pendulum length versus estimated period of oscillation of the collected data sets with fixed mass $m = 0.10\text{kg}$ and initial angle $\theta_0 = 0.22\text{rad}$. This data is approximated with a functional fit of the form $T(\ell) = A\sqrt{\ell}$, where the proportionality constant A was optimized to take on a value of $A = (1.96 \pm 0.09)\frac{\text{s}}{\sqrt{\text{m}}}$. Further, a goodness of fit estimate takes on a value of $\chi^2 = 1.94$, indicating a strong correlation. (Right) A plot of the residual values between the collected data and the associated functional forms.

To verify that the period of oscillation is independent of the masses being used, Figure 3a is generated, plotting the estimated periods for each associated weight while leaving $L = 0.1\text{m}$ and $\theta_0 = 0.22\text{rad}$ fixed. These data points are plotted alongside the constant function which takes on a value equal to that of the average period of the five data sets under consideration. There is indeed significant deviation between each singular value of T and the average value of T , however these deviations are at least an order of magnitude smaller than the magnitude of the periods themselves. Further discussion on these deviations is included in the uncertainty analysis section of this report. Observing the differentiation between the values of T for subsequent masses, it is rather clear that there is no suitable correlation between the mass and the period other than their mutual independence. Indeed if there were a relation, the period would be either increasing or decreasing with an increase in mass, neither trend of which accurately describes the behaviour present in Figure 3a. As such, this data allows for conclusivity; the period of oscillation T is independent of the mass m of the weights being used.



(a) Mass versus estimated period



(b) Initial angular amplitude versus estimated period

Figure 3: (Left) A plot of the mass versus estimated period of oscillation of the collected data sets with fixed length $L = 0.10\text{m}$ and initial angle $\theta_0 = 0.22\text{rad}$. These points are plotted alongside the constant function of magnitude equal to the average value of the estimated periods. (Right) A plot of the initial angular amplitude versus estimated period of oscillation of the collected data sets with fixed length $L = 0.10\text{m}$ and mass $m = 0.05\text{kg}$. These points are plotted alongside the constant function of magnitude equal to the average value of the estimated periods.

Finally, to verify the independence of the period T on the initial angular amplitude θ_0 , Figure 3b plots the estimated period of oscillation against the initial angular amplitude that each data set underwent. The average value of the estimated periods is plotted alongside the data points. In an effort to truly display the existence of the small angle approximation, eight (8) distinct data sets have been recorded, five of which take on initial angular amplitude less than $0.25\text{rads} \approx 15^\circ$. As is clearly evident in the generated plots, the estimated period takes on highly consistent values for the first five data sets – the collection whose initial amplitude is sufficiently small. In fact, up to uncertainty, the first five estimated periods are equal. Further increasing the initial amplitude, however, results in an increase in the period of oscillation. This trend remains consistent for all of the plot points whose initial angular amplitude exceeds 0.25rads . Hence, it is appropriate to conclude that the period of oscillation is independent of the initial amplitude, so long as the initial amplitude is sufficiently small.

Decay Constant τ

For all 16 data sets, each of which captures a full minute of oscillation, a value of the decay coefficient τ is optimized to fit the behaviour of the pendulum. In most cases, the resulting decay coefficient allows the optimized functional fit of the form Eq.(3) to perfectly decay alongside of the envelope of the recorded data. This is displayed exquisitely in Figures 6a and 6b, particularly the former of these which carries a goodness of fit estimation of $\chi^2 = 1.35$ and the

envelope of which decays by a factor of (over) $1/e$ of its initial value; this objectively proves the exponential decay in the angular amplitude of the mass over time. With that being said, a few of the functional fits did not result in optimal or expected behaviour. Examples of such fits are included in Figures 19a and 19b which clearly indicate that the functional form decays far faster than the collected data itself. This data, however, was taken with initial angular amplitudes of $\theta_0 = 0.68$ and $\theta_0 = 1.02$ respectively; relatively large angles for which the approximation that $\sin \theta \approx \theta$ used to obtain Eq.(3) itself becomes increasingly crude. These are examples where the small angle approximation fails; the level at which this approximation remains valid is discussed in further detail below.

In an effort to estimate the *efficiency* of the pendulum, the ratio of the decay coefficient to the period of oscillation is computed for the various combinations of the independent variables. The value of all such ratios are included in Table 1 in the appendix, and take on an average value of 108.02 (note that this value is a ratio of values of the same units; the ratio is unitless). If only the cases where the small angle approximation is valid are considered, this ratio takes on an average value of 119.77. These large values indicate a high level of efficiency within the system.

Naturally, the relationship between the independent variables ℓ, m, θ_0 and the decay coefficient τ are of interest. Figure 4 plots the decay coefficient for each length of pendulum, while leaving $m = 0.1\text{kg}$ and $\theta_0 = 0.22\text{rads}$ fixed, alongside two possible functional forms: one linear and one (increasing) quadratic form. Both of these fits provide decent correlation between the length of the pendulum and the decay coefficient, taking on goodness of fit estimations of $\chi^2 = 3.14$ and $\chi^2 = 2.42$ respectively. Since the quadratic form has a better goodness of fit estimation, it follows that the most likely correlation between ℓ and τ is given by

$$\tau(\ell) = (2935.98[\text{s}/\text{m}^2]) \ell^2 + (6.76[\text{s}/\text{m}]) \ell + 45.79 \quad (7)$$

Residual plots of the collected data against *both* fits are included in Figures 7a and 7b. In a similar vein, Figure 5a plots the decay coefficients for each value of the mass of the pendulum, while leaving $L = 0.10\text{m}$ and $\theta_0 = 0.22\text{rads}$ fixed. This data is plotted alongside two separately optimized functional forms: one linear form and one logarithmic form, each containing additive constants. The ladder of these plots approximates the data spectacularly having an estimated goodness of fit of $\chi^2 = 1.27$. Since the linear fit fails to obtain a goodness of fit closer to 1, it follows that the most likely correlation between m and τ is given by

$$\tau(m) = (38.90\text{s}) \log(m/(1\text{kg})) + 167.61\text{s} \quad (8)$$

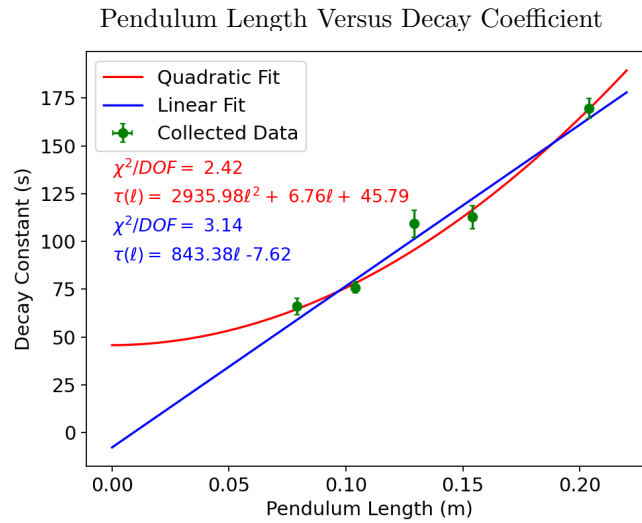
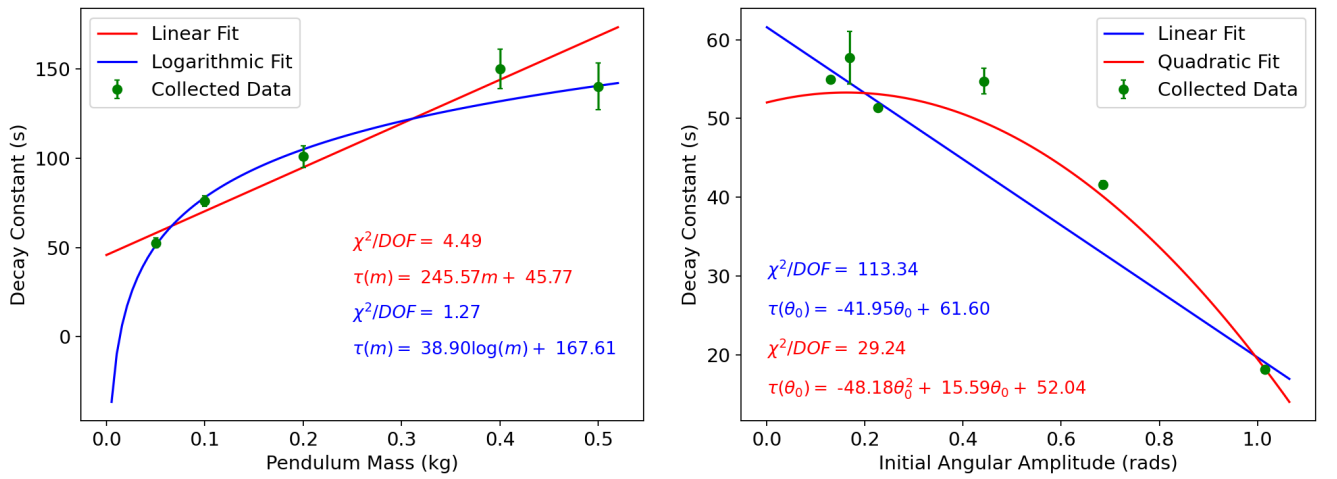


Figure 4: A plot of the various decay coefficients for the data with fixed mass $m = 0.1\text{kg}$ and initial angular amplitude $\theta_0 = 0.22\text{rads}$. This data is plotted alongside both a quadratic and linear fits, the form of each being printed onto the image, along with their respective goodness of fit estimations.

Figure 5a is accompanied by residual plots for *both* of the aforementioned functional forms given in Figures 8a and 8b in the appendix. Finally, Figure 5b plots the approximated decay coefficient for each value of the initial angular amplitude while leaving $L = 0.10\text{m}$ and $m = 0.10\text{kg}$ fixed. These data points are plotted alongside two optimized functional forms: one linear and one quadratic (both of which are decreasing on the domain of interest).



(a) Pendulum mass versus decay constant.

(b) Pendulum initial angular amplitude versus decay constant

Figure 5: Plots summarizing the estimated decay constants against the mass of the pendulum and the initial angular amplitude of the data sets respectively. These plots are included with goodness of fit estimations, as well as two possible functional forms each. The data in Figure 5a is plotted with a linear fit and a logarithmic fit, the latter of which producing the better goodness of fit estimation. The data in Figure 5b is plotted with a linear fit and a quadratic fit, the latter of which producing the better goodness of fit estimation.

Admittedly, the goodness of fits for both of these forms are extremely high, indicating a poor correlation. This is likely attributable to a lack of a sufficient number of data points as well as human error. With that being said, the quadratic fit better correlates the two variables, taking on a goodness of fit estimation of $\chi^2 = 29.24$ and has the form given by

$$\tau(\theta_0) = (-41.18[\text{s/rads}^2]) \theta_0^2 + (15.59[\text{s/rads}]) \theta_0 + 52.04 \quad (9)$$

Likewise to the above discussions, Figure 5b is accompanied by residual plots for both the optimized forms are given in Figures 9a and 9b. Note that each of the coefficients in each of the above expression (namely Eqs.(7) - (9)) carry an uncertainty value which is propagated by the covariance matrix produced by `curve_fit`, however their values are not included as it is beyond the focus of this report.

Symmetry

A perfectly symmetric simple pendulum with no damping due to drag would have the property that $\theta(t) = -\theta(t + T/2)$, for all time t where T is the period of oscillation. Any deviation from this equality implies asymmetry within the system. To quantify the asymmetry of the pendulum used to collect the data in this report, this equality is tested at each point in time t . The idea is as follows: the first 100 data points¹ of a single data set is considered and fitted with a function of the form of Eq.(3), and as such, an estimation of the period of oscillation over this set of data is obtained. This functional form is then used to obtain residuals between the functional form and the recorded data, values of which can then be averaged to obtain an average *absolute* residual value. Now shift the functional form $\theta(t)$ by an amount $T/2$ to the left, and multiply by -1: $\theta(t) \mapsto -\theta(t + T/2)$. For a perfectly symmetric pendulum, the average value of absolute residuals between the collected data and the *shifted* functional form should be precisely equal. Hence, the relative change between these two averages provides a quantitative

¹The reasoning for only using the first 100 data points is because the symmetry of the system is entirely determined after undergoing a single full oscillation anyways. The first 100 time steps include approximately four full oscillations of the pendulum, and thus this is sufficient to accurately estimate the observed level of symmetry.

estimate of the *asymmetry* of the pendulum, and subtracting this value from 1 provides a quantitative estimate of the *symmetry* of the pendulum.

Plotted in Figures 10a, 11a are the first 100 time steps of the motion of pendulum with a length $L = 0.1\text{m}$, a mass of $m = 0.1\text{kg}$ and initial angular amplitude $\theta_0 = 0.22\text{rads}$ plotted alongside a optimized functional form, and the associated residual values respectively. Plotted in Figure 10b is the same collected data, only plotted alongside the same functional form, but shifted to the left by a time $T/2 = (0.360 \pm 0.002)\text{s}$. Finally, plotted in Figure 11b is the residuals of the collected data and the *shifted* functional form. Visually, Figures 10a and 10b are extremely similar, and likewise for Figures 11a and 11b – this speaks to the high level of symmetry present in the pendulum. In fact, up to uncertainty in the angular amplitude θ , the pendulum is perfectly symmetric. With that being said, the average (absolute) residual value present in Figure 11a is 0.0048, while that of Figure 11b is 0.0049, providing a relative difference of

$$C = \frac{0.0049 - 0.0048}{0.0049} = 0.013$$

In other words, the pendulum is 1.3% asymmetric or equivalently, 98.7% symmetric: a fairly high level of symmetry. Reasons for any asymmetry at all are attributed to the effect of drag and hence the exponential decay of the envelope of the collected data.

Small Angle Approximation

The goal here is to provide a numerical domain of the initial angular amplitude for which the theory discussed in the introduction. Issues resulting from a large angular amplitude appear in the expected independence of the period of oscillation with respect to the initial angular amplitude, as well as for the validity of the functional fit of the form Eq.(3) for large initial angles. As discussed above, consistency in the estimated period (up to uncertainty) remains constant for various initial angles so long as the magnitude of the initial angle does not exceed 0.25rads. Conversely, the goodness of fit estimations for Figures (17a) through (19b) in the appendix remain reasonable up to Figure (19a), at which point the functional form does *not* accurately represent the behaviour of the data. It is thus evident that the behaviour of the pendulum follows the form of Eq.(3) for cases where the initial angular amplitude does not exceed 0.41rads (which was the initial angular amplitude of the data plotted in Figure (18b)). Taking the stricter of the two (independently obtained) conditions, a small angle approximation is valid for values of θ which lie in the domain $|\theta_0| < 0.25\text{rads}$.

Conclusion

As hypothesized in the introduction, the angular amplitude of the pendulum is governed by Eq.(3) so long as $|\theta_0| < 0.25\text{rads}$; the domain at which the small angle approximation remains valid. It is further concluded that both the mass and the angular amplitude have no impact on period of oscillation of the pendulum, so long as the small angle approximation is uniformly satisfied. A quantitative analysis of the system results in an estimated symmetry of 98.7% and a high level of mechanical symmetry, obtaining an average decay coefficient to period of oscillation quotient of 108.02. High efficiency and symmetry lead directly to minimal uncertainties and by extension, accurate results which align with the theoretical framework introduced in the introduction. Moreover, through varying the length of the pendulum ℓ (and leaving all other variables fixed) it is concluded that the period of oscillation T depends on ℓ as $T = 2\sqrt{\ell}$. Finally, the drag coefficient estimations yields data that indicates quadratically increasing, logarithmic, and quadratically decreasing dependence of τ on the length ℓ , mass m , and initial amplitude θ_0 respectively.

Bibliography

- [Lea09] Lumen Learning. “Drag Forces”. In: *ER Services* (2009).
- [Tra09] Tracker. “Tracker: Video Analysis and Modelling Tool”. In: <https://physlets.org/tracker/> (2009).
- [Ser13] Ruxandra Serbanescu. “Pendulum Project”. In: *PHY324 Labs* (2013).
- [Wik23] Wikipedia. “Propagation of Uncertainties”. In: *Wikipedia* (2023).

Appendix

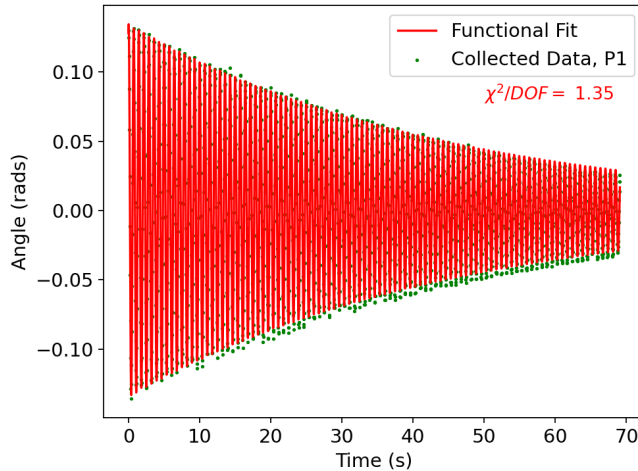
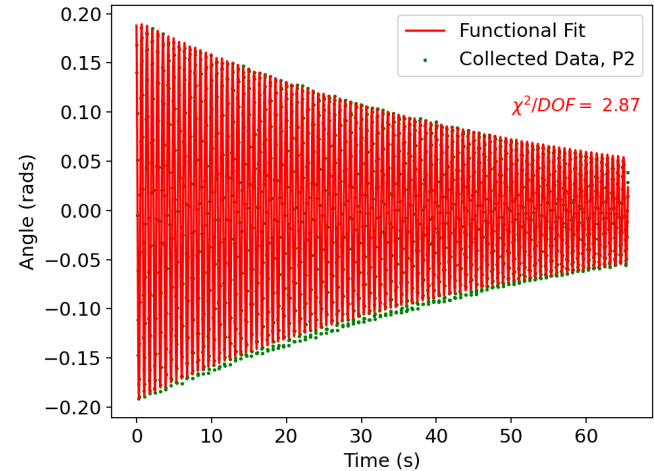
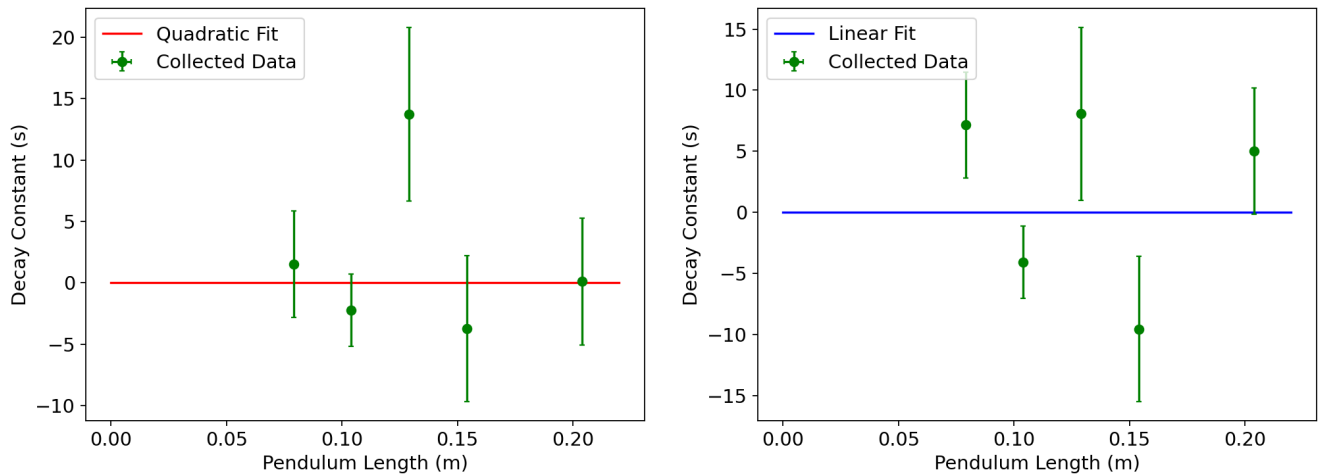
(a) $m = 0.10\text{kg}$, $L = 0.10\text{m}$, $\theta_0 = 0.13\text{rads}$ (b) $m = 0.10\text{kg}$, $L = 0.10\text{m}$, $\theta_0 = 0.19\text{rads}$

Figure 6: Plots of two sets of data which visually display the exponential decay of the amplitude of the pendulum as time evolves. The respective functional fits have a decay constant of $\tau_1 = (76.06 \pm 2.81)\text{s}$ and $\tau_2 = (51.35 \pm 0.28)\text{s}$.

Table 1: A table displaying the values of the quotient of τ/T for all of the data sets. In each column, the indicated independent variable is change, while all others are remained fixed. Note that each of the values of the ratios are numbers; these are unitless quantities used entirely for the purpose of gaining numerical estimations on the efficiency of the system. Note that only five data sets were collected where the length and mass are left fixed, while there are fix data sets with distinct angles.

Independent Variable	Data Set 1	Data Set 2	Data Set 3	Data Set 4	Data Set 5	Data Set 6
Mass m [kg]	99.73 ± 4.33	103.19 ± 2.95	135.45 ± 7.07	130.47 ± 5.96	174.21 ± 5.16	N/A
Length L [m]	73.52 ± 2.81	103.23 ± 2.95	138.32 ± 6.20	197.06 ± 11.09	186.16 ± 13.12	N/A
Amplitude θ_0 [rads]	63.13 ± 0.33	71.91 ± 0.28	80.77 ± 3.34	89.91 ± 1.64	57.12 ± 0.46	24.32 ± 0.18

Length ℓ Versus Decay Coefficient τ

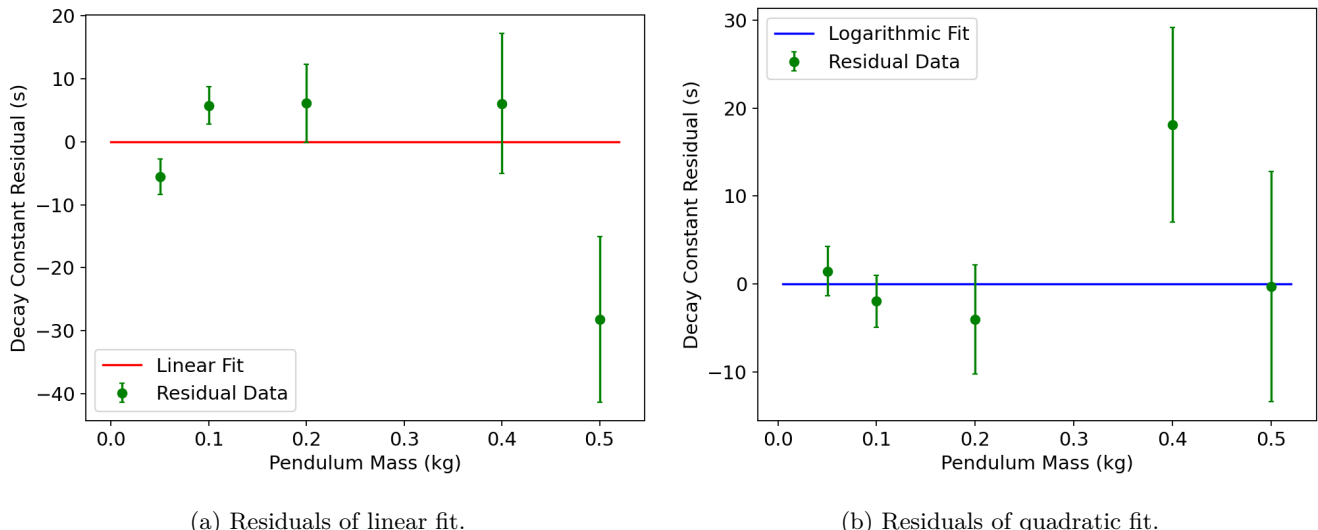


(a) Residuals of quadratic fit for length versus decay coefficient (b) Residuals of linear fit for length versus decay coefficient

Figure 7: Residual plots denoting the residuals between the period versus τ points in Figure 4 and the two functional forms fitted to the data.

Decay Coefficient τ

Mass m and Amplitude θ_0 Versus Decay Coefficient τ



(a) Residuals of linear fit.

(b) Residuals of quadratic fit.

Figure 8: Residual plots denoting the residuals between the mass versus τ points in Figure 5a and the two functional forms fitted to the data.

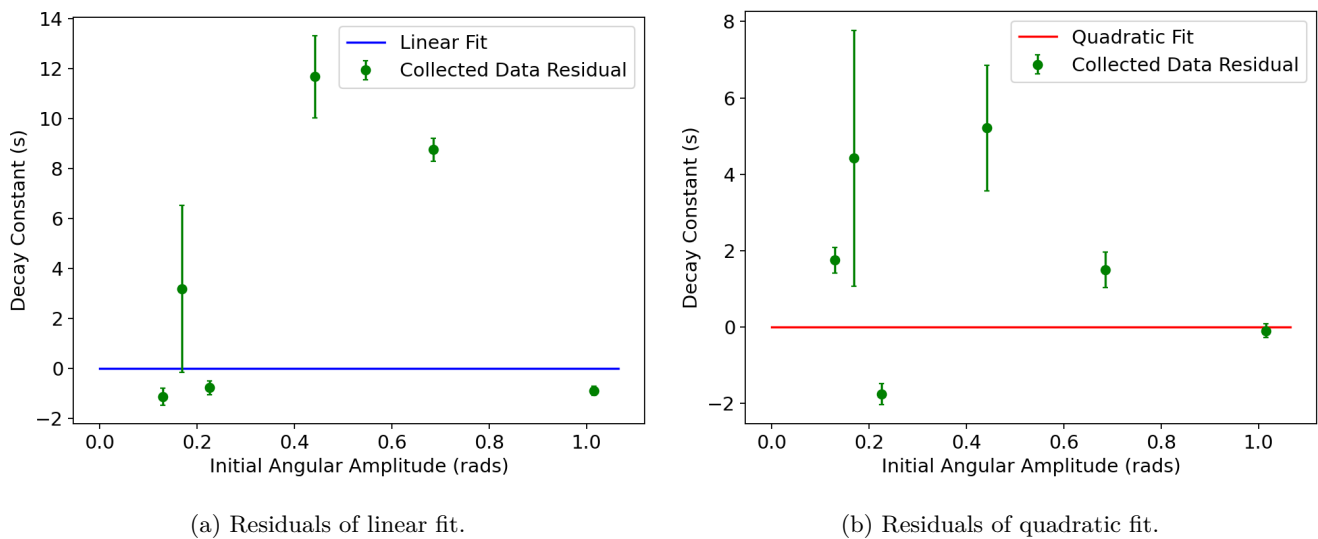


Figure 9: Residual plots denoting the residuals between the initial angular amplitude versus τ points in Figure 9 and the two functional forms fitted to the data.

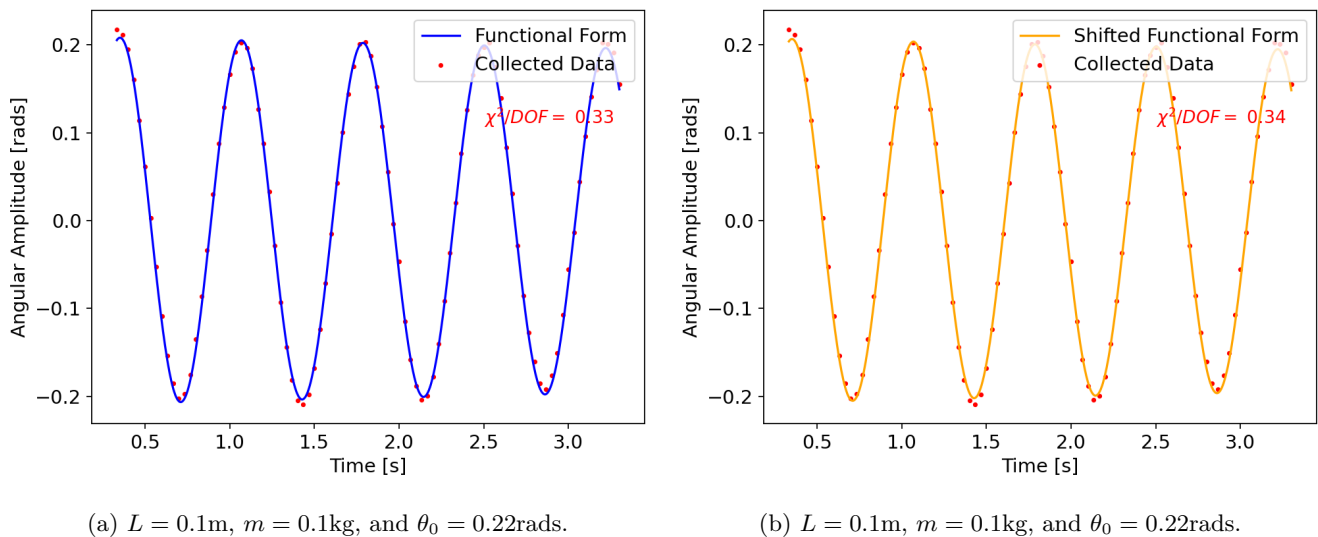
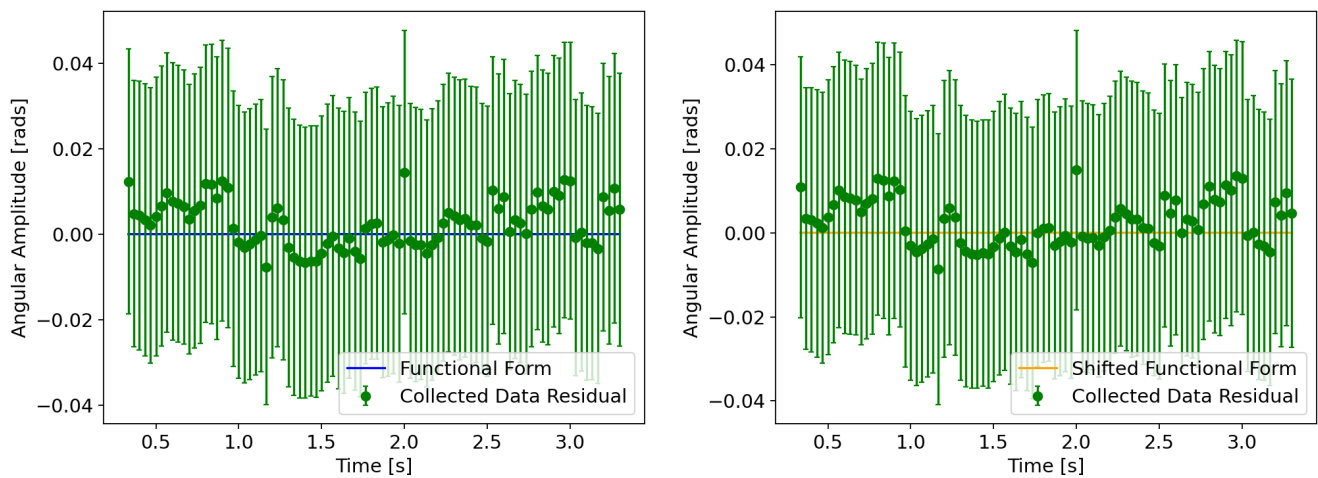


Figure 10: Two plots of the first 100 data points of the pendulum with independent variables as stated above. Figure 10a includes a functional fit of the form of Eq.(3) and is printed with it's associated goodness of fit estimation. Figure 10b contains the exact same functional form, but shifted a value $T/2 = (0.36 \pm 0.0012)$ s, and mirrored across the t axis.



(a) Residuals of collected data in Figure 10a.

(b) Residuals of collected data in Figure 10b.

Figure 11: Residual plots of the data in Figures 10a and 11a against the fitted functional form and the shifted functional form respectively.

Raw Data Plots

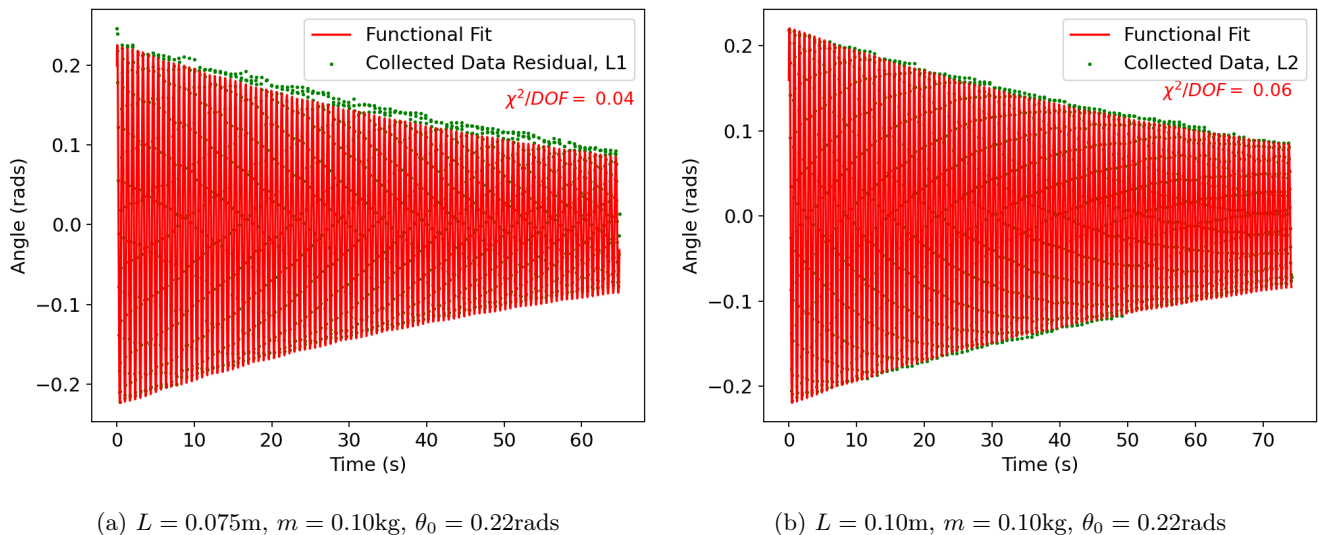
(a) $L = 0.075\text{m}$, $m = 0.10\text{kg}$, $\theta_0 = 0.22\text{rads}$ (b) $L = 0.10\text{m}$, $m = 0.10\text{kg}$, $\theta_0 = 0.22\text{rads}$

Figure 12: Plots of the angular amplitude versus time for two systems with independent variables specified above plotted alongside an optimized function of the form Eq.(3). Each data set includes over 1 full minute of behaviour of the pendulum.

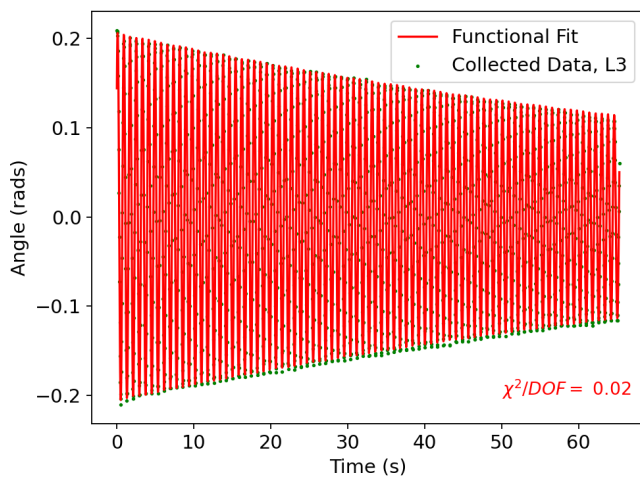
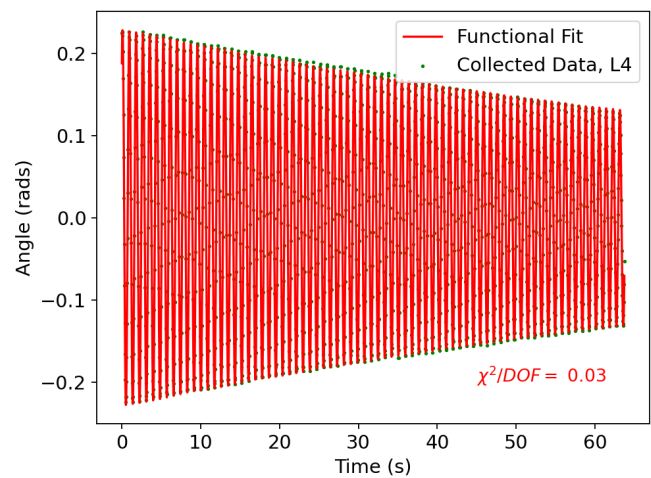
(a) $L = 0.125\text{m}$, $m = 0.10\text{kg}$, $\theta_0 = 0.22\text{rads}$ (b) $L = 0.15\text{m}$, $m = 0.10\text{kg}$, $\theta_0 = 0.22\text{rads}$

Figure 13: Plots of the angular amplitude versus time for two systems with independent variables specified above plotted alongside an optimized function of the form Eq.(3). Each data set includes over 1 full minute of behaviour of the pendulum.

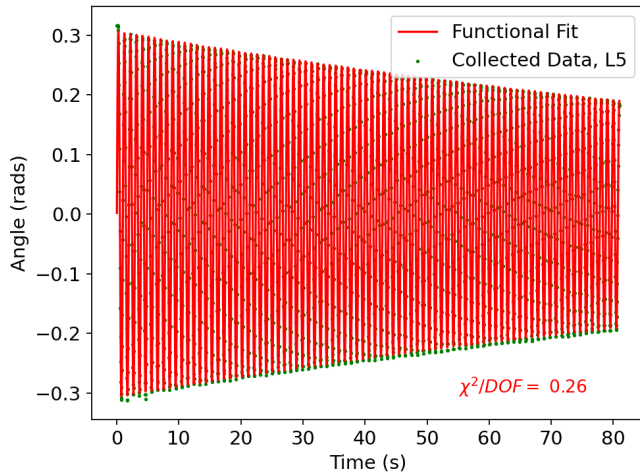
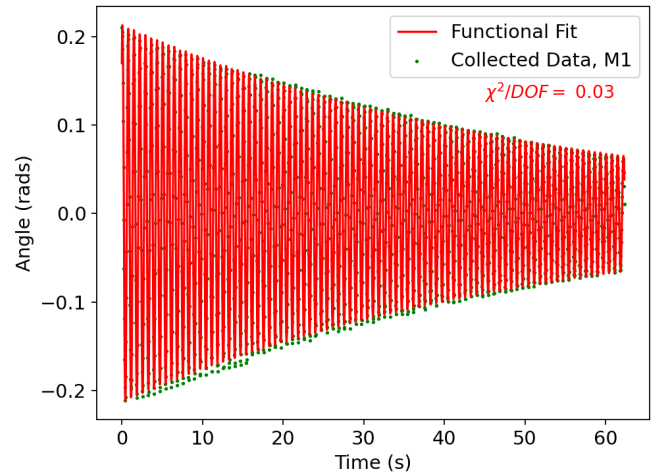
(a) $L = 0.20\text{m}$, $m = 0.10\text{kg}$, $\theta_0 = 0.22\text{rads}$ (b) $L = 0.10\text{m}$, $m = 0.05\text{kg}$, $\theta_0 = 0.22\text{rads}$

Figure 14: Plots of the angular amplitude versus time for two systems with independent variables specified above plotted alongside an optimized function of the form Eq.(3). Each data set includes over 1 full minute of behaviour of the pendulum.

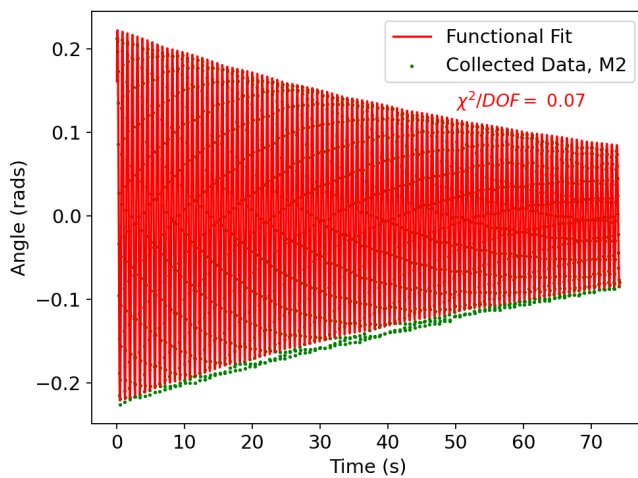
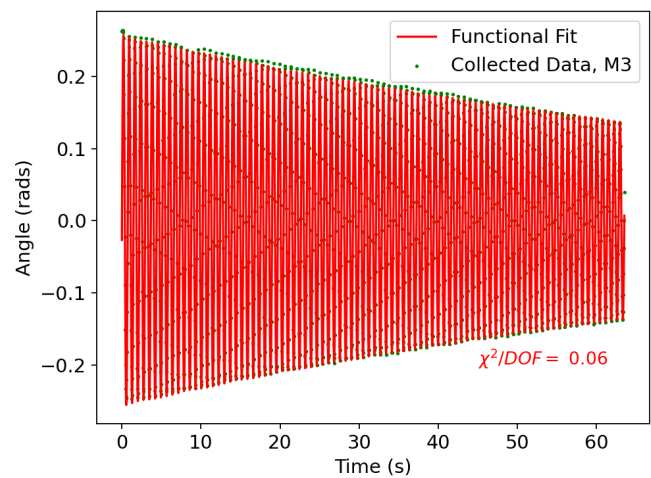
(a) $L = 0.10\text{m}$, $m = 0.10\text{kg}$, $\theta_0 = 0.22\text{rads}$ (b) $L = 0.10\text{m}$, $m = 0.10\text{kg}$, $\theta_0 = 0.22\text{rads}$

Figure 15: Plots of the angular amplitude versus time for two systems with independent variables specified above plotted alongside an optimized function of the form Eq.(3). Each data set includes over 1 full minute of behaviour of the pendulum.

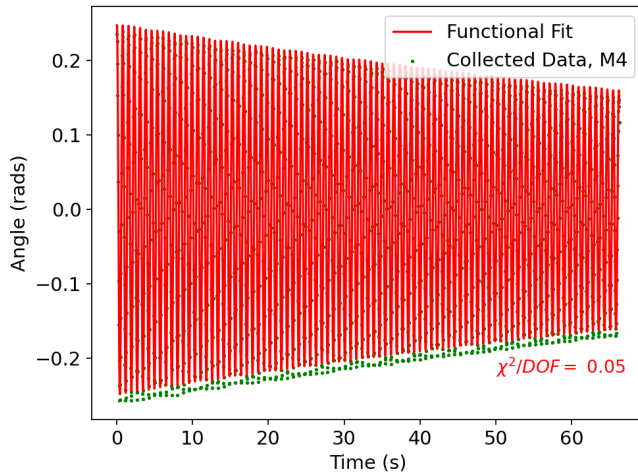
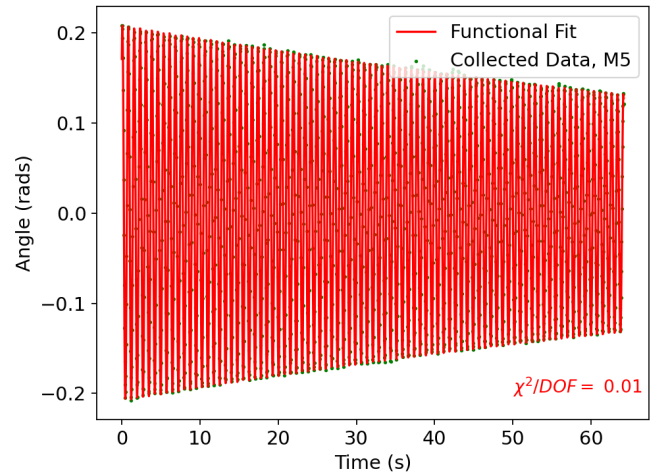
(a) $L = 0.10\text{m}$, $m = 0.20\text{kg}$, $\theta_0 = 0.22\text{rads}$ (b) $L = 0.10\text{m}$, $m = 0.40\text{kg}$, $\theta_0 = 0.22\text{rads}$

Figure 16: Plots of the angular amplitude versus time for two systems with independent variables specified above plotted alongside an optimized function of the form Eq.(3). Each data set includes over 1 full minute of behaviour of the pendulum.

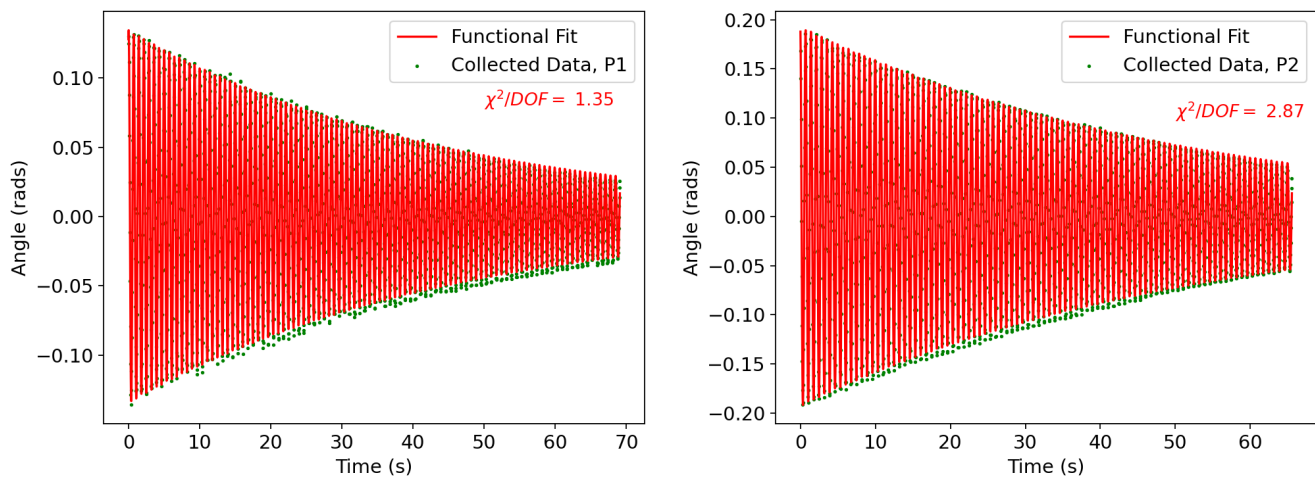


Figure 17: Plots of the angular amplitude versus time for two systems with independent variables specified above plotted alongside an optimized function of the form Eq.(3). Each data set includes over 1 full minute of behaviour of the pendulum.

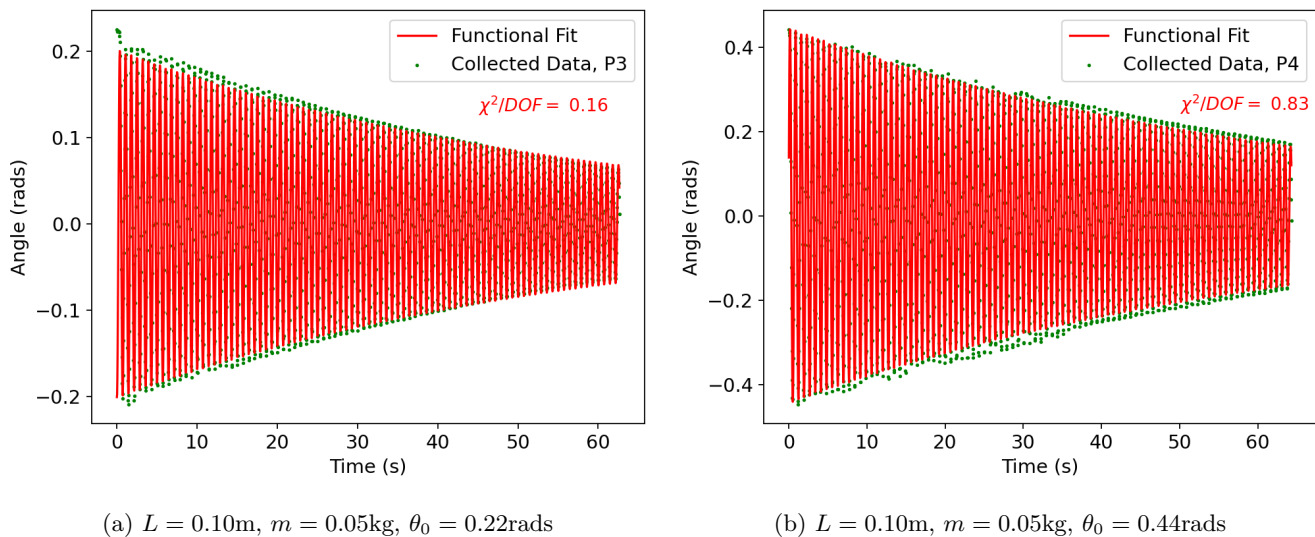


Figure 18: Plots of the angular amplitude versus time for two systems with independent variables specified above plotted alongside an optimized function of the form Eq.(3). Each data set includes over 1 full minute of behaviour of the pendulum.

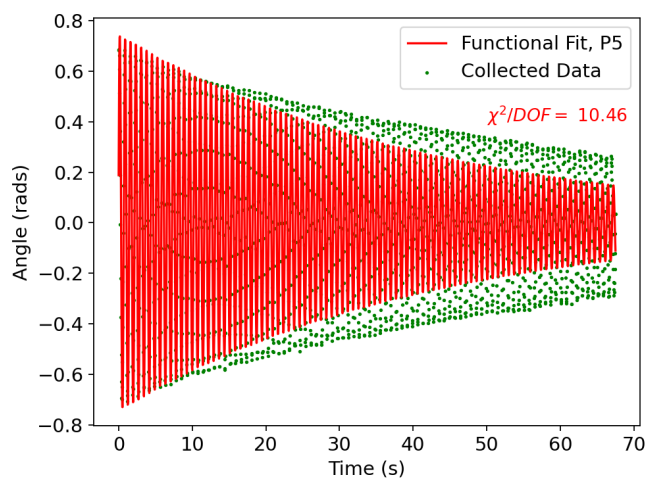
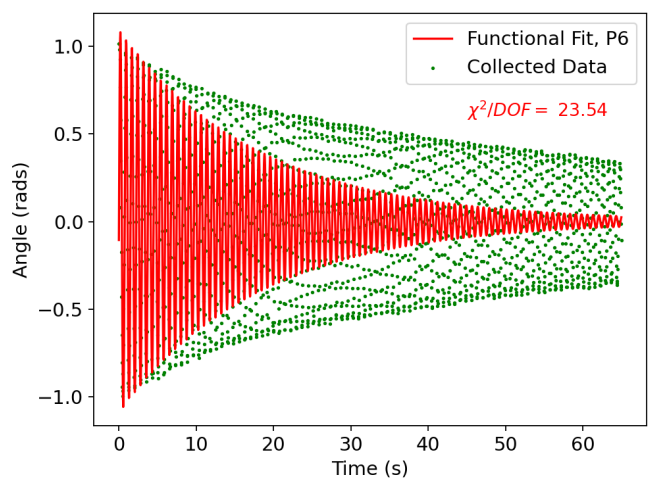
(a) $L = 0.10\text{m}$, $m = 0.05\text{kg}$, $\theta_0 = 0.68\text{rads}$ (b) $L = 0.10\text{m}$, $m = 0.05\text{kg}$, $\theta_0 = 1.02\text{rads}$

Figure 19: Plots of the angular amplitude versus time for two systems with independent variables specified above plotted alongside an optimized function of the form Eq.(3). Each data set includes over 1 full minute of behaviour of the pendulum.